Modelling of pressure gradient in the space behind the projectile

Luděk JEDLIČKA, Stanislav BEER, Miroslav VÍDEŇKA
Department of weapons and ammunition
University of Defence
Kounicova 65, 615 00 BRNO 15
Czech Republic

Abstract: -The article deals with modelling of pressure distribution of propellant gases in the space behind the projectile of ordinary ballistic system. The number of existing models describing the pressure gradient is analyzed and confronted with results of experimental firings carried out on the high performance anti-aircraft cannon of calibre of 30 mm.

Key-Words: - ballistics, interior ballistics, pressure gradient, projectile base pressure, breech pressure

1 Introduction

During the movement of a projectile inside a barrel is created a pressure gradient between the barrel breech and the projectile base due to the difference in velocities of propellant gases at the breech and the projectile base, Fig. 1. This pressure gradient belongs among factors that significantly affect not only interior ballistic calculations but also the design of projectiles. The pressure gradient is usually characterized by the ratio of the breech pressure p_d and the projectile base pressure p_s.

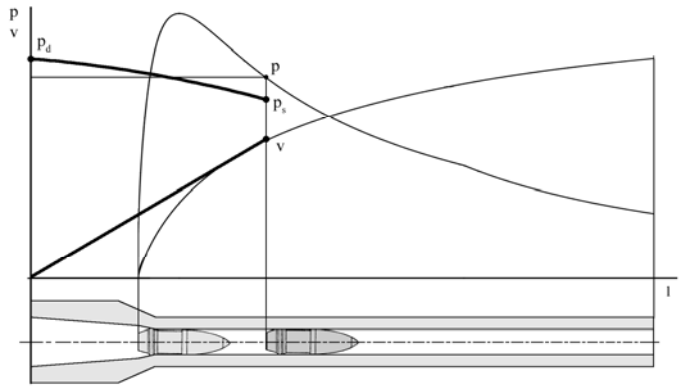

Fig. 1 Pressure gradient in the space behind a projectile
p... ballistic pressure, v... velocity of projectile,
l... projectile trajectory

The literature [1], [7] contains number of models describing the pressure gradient but without any comparison with experimental results. Most of the models are relatively old and were created for ballistic systems of lower performance, e.g. howitzers. There is not any study analysing the suitability of these models for modern medium calibre and high performance ballistic systems that still satisfy the condition $\omega / m_q < 1$.

2 Models of pressure gradient

From above mentioned literature four the most widespread models describing the pressure gradient in the space behind a projectile were chosen and were marked for needs of this article as Model 1 – 4. The fifth pressure distribution model is used in the interior ballistic model described in [3] and was marked as model STANAG 4367.

Generally, it can be said, that basic element of all analysed models of pressure gradient is the ratio $\frac{\omega}{2\,m_q}$,

where:
ω… mass of propellant charge,
m_q… mass of the projectile.

2.1 Model 1

This model is determined for ballistic systems with a cylindrical cartridge chamber of the same area of cross-section as area of cross-section of barrel, Fig. 2.

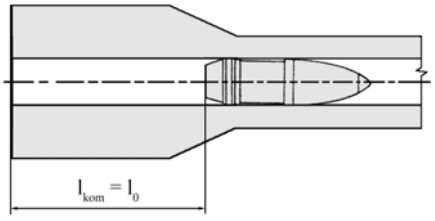

Fig. 2 Schema of cylindrical cartridge chamber ($l_{kom} = l_0$)
l_{kom} … length of cartridge chamber,
l_0… length of initial combustion volume

In this model is the ratio of breech pressure to the projectile base pressure expressed as

$$\frac{p_d}{p_s} = 1 + \frac{\omega}{2\,\varphi_1\,m_q}, \qquad (1)$$

where:
p_d ... breech pressure,
p_s ... projectile base pressure,
ω ... mass of propellant charge,
m_q ... mass of projectile,
φ_1 ... losses coefficient (usually between 1.02 (howitzers and cannon) and 1.1 (small arms 1.05 – 1.1), [7], [8]).

In this model the ratio p_d / p_s strongly depends only on ratio ω / m_q and remains constant during the projectile movement inside the barrel, i.e. the ratio is independent of the projectile trajectory. The dependency for common extent of values ω / m_q is shown in Fig. 3.

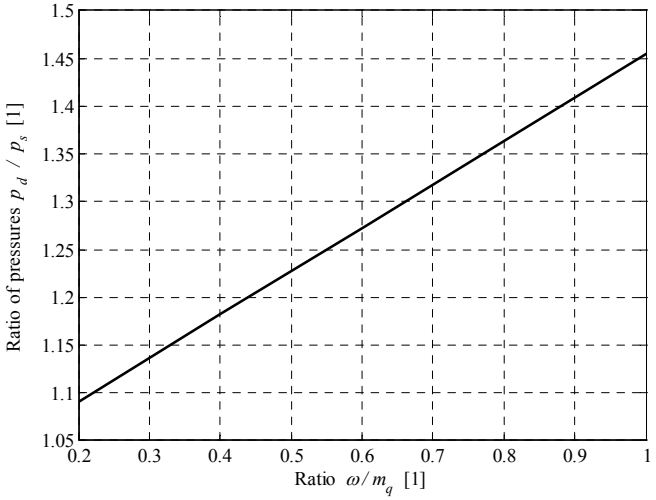

Fig. 3 Dependency of p_d / p_s on ratio ω / m_q
$\varphi_1 = 1.1$

From the Fig. 3 is clearly seen that according to the Model 1 is the pressure ratio p_d / p_s directly proportional to the ratio ω / m_q.

2.2 Model 2

A real cartridge chamber has usually bigger diameter than the diameter of the barrel. This model is based on the Model 1 and extended by an effect of cartridge chamber shape. The effect of the cartridge chamber shape is described by the coefficient of cartridge chamber shape $\chi = \frac{l_0}{l_{kom}}$, Fig. 4.

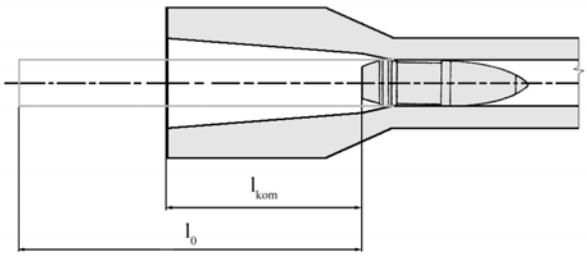

Fig. 4 Schema of real cartridge chamber ($l_{kom} \neq l_0$)

The ratio of breech pressure p_d to the projectile base pressure p_s is, in this model, described by following empirical relation

$$\frac{p_d}{p_s} = \left(1 + \frac{\omega}{2\,\varphi_1\,m_q}\right) \cdot \left(\frac{1}{\chi}\right)^k, \qquad (2)$$

where:
χ ... coefficient of cartridge chamber shape,
k ... exponent (recommended value 0.3,[1]).

For calculation of exemplary courses of p_d / p_s were chosen typical extent of ratios ω / m_q from 0.2 to 1.0, exponent k = 0.3 according to recommendations from literature, and coefficient φ_1 = 1.1. The obtained dependencies of p_d / p_s are shown in Fig. 5.

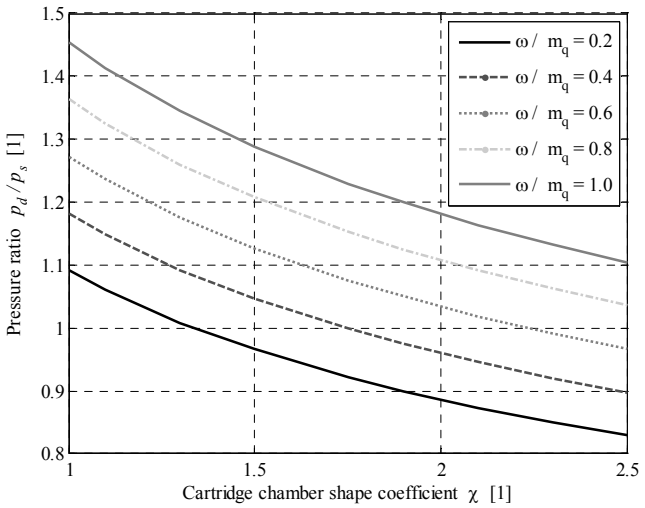

Fig. 5 Dependency of p_d / p_s on cartridge chamber shape coefficient χ
$\varphi_1 = 1.1$, $k = 0.3$

The ratio p_d / p_s is again independent of the projectile trajectory and remains constant during the projectile movement inside the barrel. Generally, the ratio p_d / p_s decreases with increasing cartridge chamber shape coefficient χ and with decreasing ratio ω / m_q.

Further the figure shows that there are, according to this model, certain combinations of cartridge chamber shapes coefficients χ and ratios ω / m_q that gives p_d / p_s

smaller than 1; in other words the breech pressure would be lower than the projectile base one. This fact is, in case of classical ballistic systems satisfying the condition $\omega / m_q < 1$, unexplainable.

2.3 Model 3

The Model 3 is also based on the Model 1. This time the Model 1 is extended not only by the effect of the shape of cartridge case chamber χ but also by the effect of increasing volume of the space behind the projectile expressed by the projectile trajectory l and the pressure gradient is written as

$$\frac{p_d}{p_s} = 1 + \frac{\omega}{2\,\varphi_1\,m_q} \cdot \left(1 - \frac{\chi - 1}{\chi \left(1 + \frac{s\,l}{c_0} \right)^3} \right), \qquad (3)$$

where:
s ... cross-sectional area of barrel,
c_0 ... initial volume of cartridge chamber.

The ratio p_d / p_s was calculated again for typical values and is shown in Fig. 6. From the figure is clearly seen that p_d / p_s increases with the trajectory of the projectile and also with ratio ω / m_q. The increase of p_d / p_s is the steepest in the beginning of projectile movement and later becomes nearly constant.

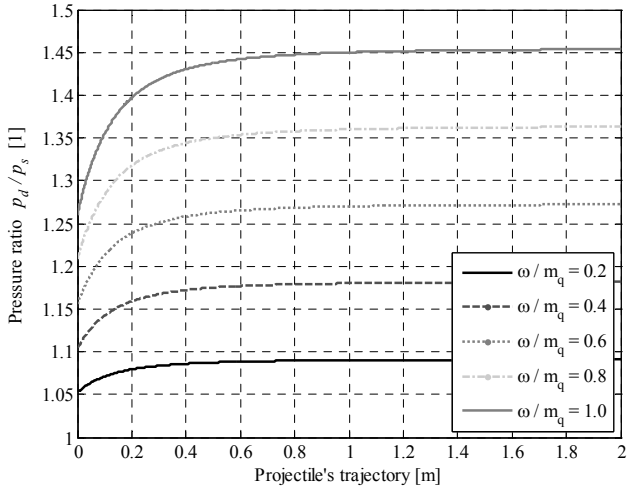

Fig. 6 Dependency of p_d / p_s on projectile's trajectory $\varphi_1 = 1.1$, $c_0 / s = 0.4$, $\chi = 1.75$

2.4 Model 4

As a last of the most used models of the pressure gradient in the space behind the projectile that takes into account except ω and m_q, also χ and relative projectile trajectory Λ. The ratio p_d / p_s is given by following relation

$$\frac{p_d}{p_s} = 1 + \frac{\omega}{2\,\varphi_1\,m_q} \cdot \left(1 - \frac{1 - \frac{1}{\chi^2}}{(1 + \Lambda)^2} \right) \qquad (4)$$

where: $\Lambda = \dfrac{s\,l}{c_0}$.

For calculation was again chosen the typical extent of ratios ω / m_q from 0.2 to 1.0. The obtained dependencies are shown in Fig. 7. The figure shows that p_d / p_s increases with the trajectory of the projectile and also with ratio ω / m_q. The increase of p_d / p_s is again the steepest at the beginning of projectile movement.

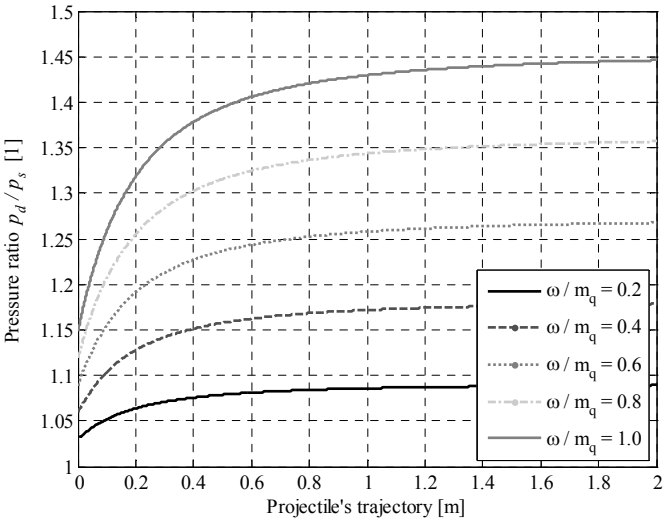

Fig. 7 Dependency of p_d / p_s on projectile's trajectory $\varphi_1 = 1.1$, $c_0 / s = 0.4$, $\chi = 1.75$

2.5 Model STANAG 4367

In the Model STANAG 4367 that is a part of the interior ballistic model described in [3] is the ratio p_d / p_s given by the following relation

$$\frac{p_d}{p_s} = 1 + \frac{\omega}{2\,m_q} \cdot \left(1 - \frac{p_R}{p_s} - \frac{p_g}{p_s} \right), \qquad (5)$$

where:
p_R ... resistance pressure against projectile motion,
p_g ... pressure of gases ahead of projectile.

It can be seen that the ratio p_d / p_s depends not only on ω and m_q but also on ratios p_R / p_s and p_d / p_s. All variables, with exception of ω and m_q, are time dependent, and so the ratio p_d / p_s is not constant during

projectile movement inside the barrel. Typical course of ratio p_d / p_s on projectile's trajectory is shown in Fig. 8.

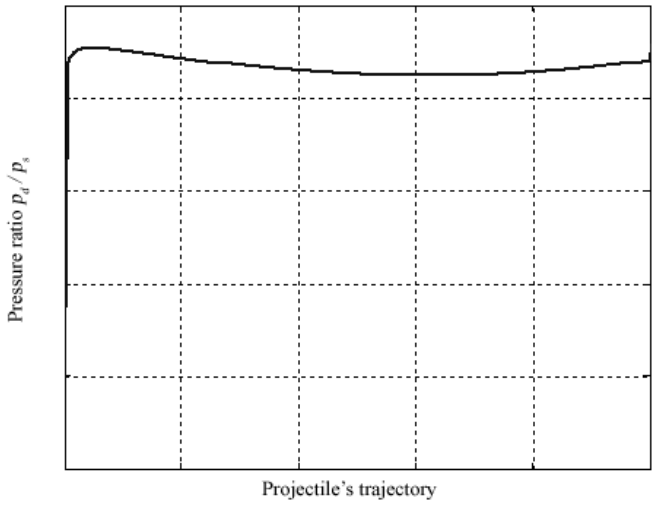

Fig. 8 Dependency of p_d / p_s on projectile's trajectory

All previously analyzed models were used for calculation of ratios p_d / p_s for a ballistic systems of calibre of 30 mm that was later also used for experiments. Its ballistic characteristics were $\omega = 0.185$, $m_q = 0.389$ kg, $\chi = 1.9$, $\varphi_1 = 1.03$, $c_0 = 2.319\text{e-}4$ m^3, $s = 7.364\text{e-}4$ m^2. Obtained theoretical results are summarized in Table 1. Distances of individual pressure gauges from back of barrel are shown in Fig. 9.

Table 1 Results of calculations of p_d / p_s from individual models

Gauge No.	2	3	4	5	6
Model 1	1.23	1.23	1.23	1.23	1.23
Model 2	1.01	1.01	1.01	1.01	1.01
Model 3	1.16	1.22	1.23	1.23	1.23
Model 4	1.11	1.19	1.22	1.22	1.23
Model STANAG 4367	1.22	1.22	1.21	1.21	1.22

3 Experiments

For the validation of all previously mentioned models of the pressure gradient in the space behind the projectile it is necessary to know the breech pressure p_d and the projectile base pressure p_s. The experiment was focused on the measurement of the pressure of propellant gases at the breech and at the base of the projectile.

The measurement of the projectile base pressure was realized by means of five piezoelectric pressure gauges placed along the barrel, Fig. 9. The projectile base pressure was read when the projectile passed the individual pressure gauges.

For the experiment the ballistic testing weapon of caliber of 30 mm based on anti-aircraft gun 30 mm PLDvK M 53 was used. For the test firings was used practice ammunition 30 mm JNhSv, $v_0 = 1000$ m.s^{-1}. The schema of used ballistic barrel with positions of piezoelectric pressure gauges is shown in Fig. 9.

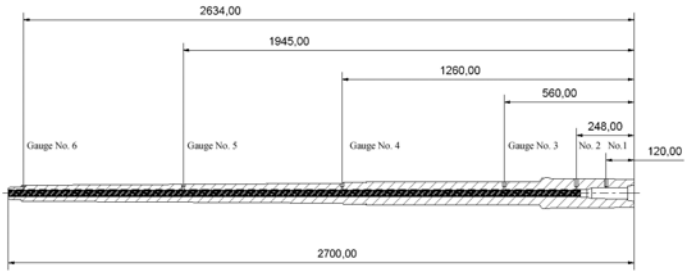

Fig. 9 Schema of ballistic barrel with positions of pressure gauges

Example of measured pressures on all pressure gauges is shown in Fig. 10.

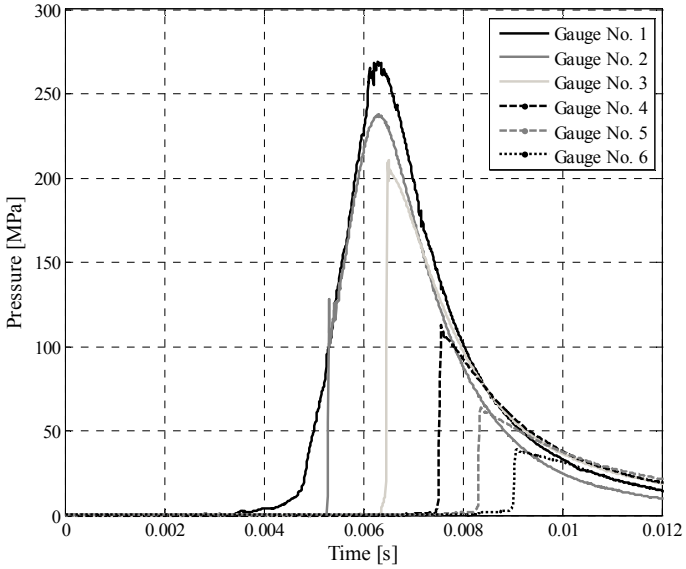

Fig. 10 Example of measured pressures

4 Results of experiments their analysis

From obtained experimental data were determined pressures at individual gauges (Gauges No. 2 - 6) at instant of projectile's arrival p_s and their corresponding breech pressures p_d (Gauge No. 1). The evaluated values of both pressures together with corresponding pressure ratios p_d / p_s are summarized in Table 2.

Table 2 Results of experimental firings

Gauge No.	2	3	4	5	6
p_d [MPa]	100.45	246.77	130.77	78.27	51.18
p_s [MPa]	100.45	201.68	108.41	63.55	38.09
p_d / p_s [1]	1.00	1.22	1.21	1.23	1.34

Calculated and experimentally obtained ratios p_d / p_s are compared in Fig. 11. At experimentally obtained ratios p_d / p_s are also shown their corresponding standard deviations.

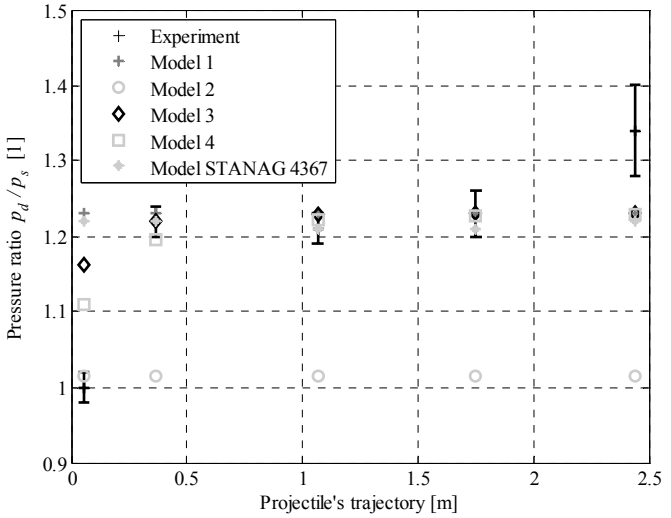

Fig. 11 Comparison of experimental and calculated p_d /p_s

From comparison of results of calculations and experimentally obtained p_d / p_s follows that the results of calculations are in good agreement with experiment data, especially in the middle part of the barrel. The only exception is the Model 2 whose results do not agree neither with results of experiment nor with results of other models. This disagreement is caused by inappropriate value of the exponent k. From the comparison can be further seen that at the beginning of projectile motion and near the muzzle is the difference between results of calculations and experiments more significant.

5 Conclusion

The bigger difference between measured and calculated ratios p_d / p_s near the muzzle of the barrel can be explained by the leak of propellant gases between barrel wall and driving band that is at this stage of projectile movement worn. Barrel wear usually also grows towards the muzzle of barrel.

Common disadvantage of all the analysed models is the fact that none of them takes into account the leakage of propellant gases. In other words, due to wear of the driving band is changed the contact pressure between the driving band and the barrel wall.

The Model 2 requires more suitable value of the exponent k to get into better agreement with experimental results.

References:

[1] SEREBRJAKOV, M. E. *Interior ballistics*. 2nd Edition. Moskva: Oborongiz, 1949.

[2] VENTCEL, D. A. *Interior ballistics*. Praha: Státní nakladatelství technické literatury, 1953.

[3] STANAG 4367 *Interior ballistic model with global parameters*.

[4] *Interior ballistics of guns*. editor KRIER, H. New York: American institute of aeronautics and astronautics, 1979. ISBN 0915928329.

[5] *Gun propulsion technology*. editor STIEFEL, L. Washington DC: American institute of aeronautics and astronautics, 1988. ISBN 0930403207.

[6] *Textbook of ballistics and gunnery*. editor LONGDON, L. W., London: Her Majesty's stationery office, 1987.

[7] PLÍHAL, B., JEDLIČKA, L. *Use of hydrodynamic principle in thermodynamic interior ballistic model*. [Textbook]. Brno: Military academy in Brno, 2003.

[8] PLÍHAL, B., BEER, S., JEDLIČKA, L. *Interior ballistics of barrel weapons*. [Textbook]. 1st Edition. Brno: University of Defence, 2004. 350 s. ISBN 80–85960–83–4.

[9] GUBAREV, A., VILJUNOV, V., N., MEDVEDĚV, Ju., J. *Thermodynamic basics of interior ballistics of barrel weapons*. Penza: PVAUI, 1974.

[10] ČURBANOV, Je., V. *Interior ballistics*. Leningrad: VAA, 1975.